Journal of Magnetism and Magnetic Materials 65 (1987) 151–158
North-Holland, Amsterdam

HYSTERESIS AND ROTATIONAL HYSTERESIS OF TEXTURED POLYCRYSTALLINE MAGNETS

K. ELK and V. CHRISTOPH

Hochschule für Verkehrswesen "Friedrich List", Wissenschaftsbereich Physik, Dresden, GDR

Received 29 July 1986

A system of magnetic particles with uniaxial anisotropy is considered. The orientation of the particles is described by a distribution function, representing the texture by a single integer n. In each particle, two elementary processes of the magnetization reversal of the particles are taken into account, the coherent rotation of the magnetization and the pinning of domain walls. In the framework of this model the hysteresis loops including minor loops and virgin curves and the rotational hysteresis are computed, where arbitrarv angles between the texture axis and the external field are taken into consideration.

1. Introduction

The magnetic properties of polycrystalline fine particle magnets are mainly determined by single-particle properties (single particle hysteresis loop, saturation magnetization M_S and crystal anisotropy K_1) and the distribution of the easy axes of the particles (texture). Assuming the single particle properties to be given, the resulting magnetic properties of the ensemble can be calculated by averaging the single-particle magnetizations over a given texture function. However, this approach is justified only for high coercive permanent magnets where because of $K_1 \gg M_S^2/\mu_0$, magnetostatic interaction effects between the particles can be neglected.

In the present paper the magnetic properties of a system of non-interacting identical uniaxial particles with a given distribution of the easy axes are calculated numerically. Contrary to recent papers [1–4] no additional assumptions are made on the strength of the magnetic field and its orientation with respect to the texture axis. Hysteresis loops for different orientations of the magnetic field (including minor loops) and torque curves are calculated. Comparing characteristic values of the calculated loops with experimental measured ones, information on magnet parameters as the degree of texture can be obtained.

2. Model

2.1. Elementary processes of remagnetization

Applying an external magnetic field, the magnetization of the sample can be changed by coherent as well as incoherent magnetization processes. To determine the coherent magnetization changes in a homogeneously magnetized particle with uniaxial anisotropy K_1 the magnetic free energy

$$F(\varphi) = K_1 \sin^2\varphi - HM_S \cos(\vartheta - \varphi) \qquad (1)$$

has to be minimized with respect to the angle φ between the easy axis of the particle and the particle magnetization (cf. fig. 1). In general, there

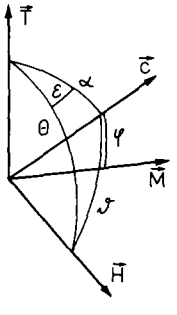

Fig. 1. Definition of the used angles. $\boldsymbol{T}$ – texture axis, $\boldsymbol{H}$ – magnetic field, $\boldsymbol{c}$ – easy direction and $\boldsymbol{M}$ – magnetization of a given crystallite.

are two solutions φ_ν ($\nu = 1,2$) with $0 \le \varphi_1 \le \pi/2 \le \varphi_2 \le \pi$. A solution φ_ν is stable if $\partial^2 F(\varphi_\nu)/\partial\varphi_\nu^2 > 0$. For magnetic fields $H < H_A/2$ ($H_A \equiv 2K_1/M_S$) both solutions are stable with respect to coherent magnetization reversals. For $H > H_A$ only one solution exists, whereas for intermediate fields $H_A/2 < H < H_A$ two solutions exist only in a definite range of angles ϑ depending on H.

On the other hand, we have to include an incoherent magnetization reversal by a shift of a Bloch wall within a given crystallite. According to Kondorsky [5] we assume that a wall shift leads the crystallite from one homogeneously magnetized state immediately to the other possible state with almost opposite magnetization, i.e. for a crystallite with an easy axis parallel to the field direction the hysteresis loop is rectangular. The incoherent magnetization reversal takes place if the component of the external field antiparallel to the easy direction of the crystallite, $H|\cos\vartheta|$, exceeds a critical value H_c^0, i.e. if

$$H \ge H_c^0/|\cos\vartheta|. \tag{2}$$

H_c^0 is an empirical parameter which describes the real structure of the particle. For all existing hard magnetic materials the Kondorsky parameter H_c^0 is much smaller than the anisotropy field $H_A = 2K_1/M_S$, i.e. $h_c^0 \equiv H_c^0/H_A \ll 1$ [6,7]. In the following we assume h_c^0 as to be given and, for definiteness, we take $h_c^0 = 0.1$.

If both magnetization configurations φ_1 and φ_2 are stable with respect to a coherent as well as to an incoherent magnetization reversal, the actual magnetic state of the crystallite is given by its magnetic prehistory, i.e. the crystallite remains in that magnetic state $\nu = 1$ or 2 which has been realized before.

2.2. Texture

To describe the distribution of the easy axes of the considered ensemble of identical uniaxial particles (crystallites), different ansatzes for texture functions can be used. In this paper we restrict ourselves to the fairly simple distribution function (cf. refs. [8,9])

$$f(\alpha) = (2n+1)\cos^{2n}\alpha, \quad \int_0^{\pi/2} f(\alpha)\sin\alpha\,\mathrm{d}\alpha = 1, \tag{3}$$

where α denotes the angle between the easy axis of a given crystallite and the texture axis. The distribution (3) can be generalized easily as

$$f(\alpha) = \sum_n C_{2n}(2n+1)\cos^{2n}\alpha, \quad \sum_n C_{2n} = 1. \tag{4}$$

To investigate the texture dependence of the macroscopic magnetic characteristics of the particle ensemble in this paper $n = 0$ (isotropic sample) and $n = 1$, 5, 10 are investigated. It easily can be shown that the shape of the hysteresis loops for magnetic fields parallel to the texture axis and Kondorsky parameters $h_c^0 \ll 1$ is almost independent of n for $n > 5$.

2.3. Geometrical relations

For convenience of the numerical calculations we define the angles between external field $\boldsymbol{H}$, texture axis $\boldsymbol{T}$, easy axis $\boldsymbol{c}$ and magnetization $\boldsymbol{M}$ of a given particle as shown in fig. 1, where $\boldsymbol{H}$, $\boldsymbol{c}$ and $\boldsymbol{M}$ are coplanar. To calculate a macroscopic property of the sample we have to average over the angles α and ϵ ($0 \le \alpha \le \pi/2$; $0 \le \epsilon \le 2\pi$) with the distribution function $f(\alpha)$.

For a given direction of the magnetic field the angles ϑ and φ depend on α and ϵ. By a simple geometry we find

$$\cos\vartheta = \cos\alpha\cos\theta + \sin\alpha\sin\theta\cos\epsilon, \tag{5}$$

whereas φ can be determined as discussed in section 2.1. Then the macroscopic (averaged) magnetization components parallel and perpendicular to the magnetic field, $M_\parallel$ and $M_\perp$, respectively, are given by

$$\begin{aligned} M_\parallel &= M_S \int \mathrm{d}\alpha \sin\alpha\, f(\alpha) \int \frac{\mathrm{d}\epsilon}{2\pi} \\ &\quad \times \sum_\nu W_\nu(\alpha,\epsilon)\cos(\vartheta - \varphi_\nu), \\ M_\perp &= M_S \int \mathrm{d}\alpha \sin\alpha\, f(\alpha) \int \frac{\mathrm{d}\epsilon}{2\pi} \\ &\quad \times \sum_\nu W_\nu(\alpha,\epsilon)\sin(\vartheta - \varphi_\nu) \\ &\quad \times (\cos\alpha\sin\theta - \sin\alpha\cos\theta\cos\epsilon)/\sin\vartheta. \end{aligned} \tag{6}$$

In (6) the φ_ν are functions of ϑ and H. The

prehistory of the sample (cf. section 2.1.) is described by the probability coefficients $W_\nu(\alpha, \epsilon)$ where $\Sigma_\nu W_\nu(\alpha, \epsilon) = 1$. $W_\nu(\alpha, \epsilon)$ denotes the probability that the crystallites with easy axes oriented in the direction α, ϵ are in the state ν. If only one solution $\varphi_\nu(\alpha, \epsilon)$ for given angles α, ϵ and field H is stable then the related $W_\nu(\alpha, \epsilon)$ is equal 1.

The angle ϑ is given by (5). Hence, $M_\parallel$ and $M_\perp$ depend on H, θ, the degree of texture and the magnetic prehistory of the ensemble of crystallites.

2.4. Initial states

As shown above, for the calculation of the magnetization components $M_\parallel$, $M_\perp$ we have to determine the coefficients $W_\nu(\alpha, \epsilon)$ in the initial states from which the numerical calculations are started. For the states following in the magnetization process the $W_\nu(\alpha, \epsilon)$ change as a consequence of the coherent or incoherent magnetization jumps as discussed in section 2.1. In this paper we consider the following initial states:

I) Sample in a remanence state after magnetical saturation, i.e.

$$W_1(\alpha, \epsilon) = \begin{cases} 1 \\ 0.5 \\ 0 \end{cases} \quad \text{for} \quad \vartheta \begin{matrix} < \\ = \\ > \end{matrix} \pi/2 \qquad (7)$$

(in the figures that initial state is denoted by "max").

II) Virgin state with stochastic distribution of the particle magnetizations, i.e. $W_\nu(\alpha, \epsilon) = \frac{1}{2}$ (state is denoted by "new").

III) Sample macroscopically demagnetized in an opposite field after magnetic saturation, $W_\nu(\alpha, \epsilon)$ have to be calculated numerically starting from state I.

IV) Partially magnetized states to compute minor loops. To calculate $W_\nu(\alpha, \epsilon)$ we start from the virgin state II and apply the maximum field $H < H_A$ for the considered inner loop. For $H > H_A$ state I is obtained.

3. Hysteresis loops

3.1. Magnetization and magnetization remanence

In figs. 2a, b, c hysteresis loops obtained in the model discussed in section 2 are plotted for differ-

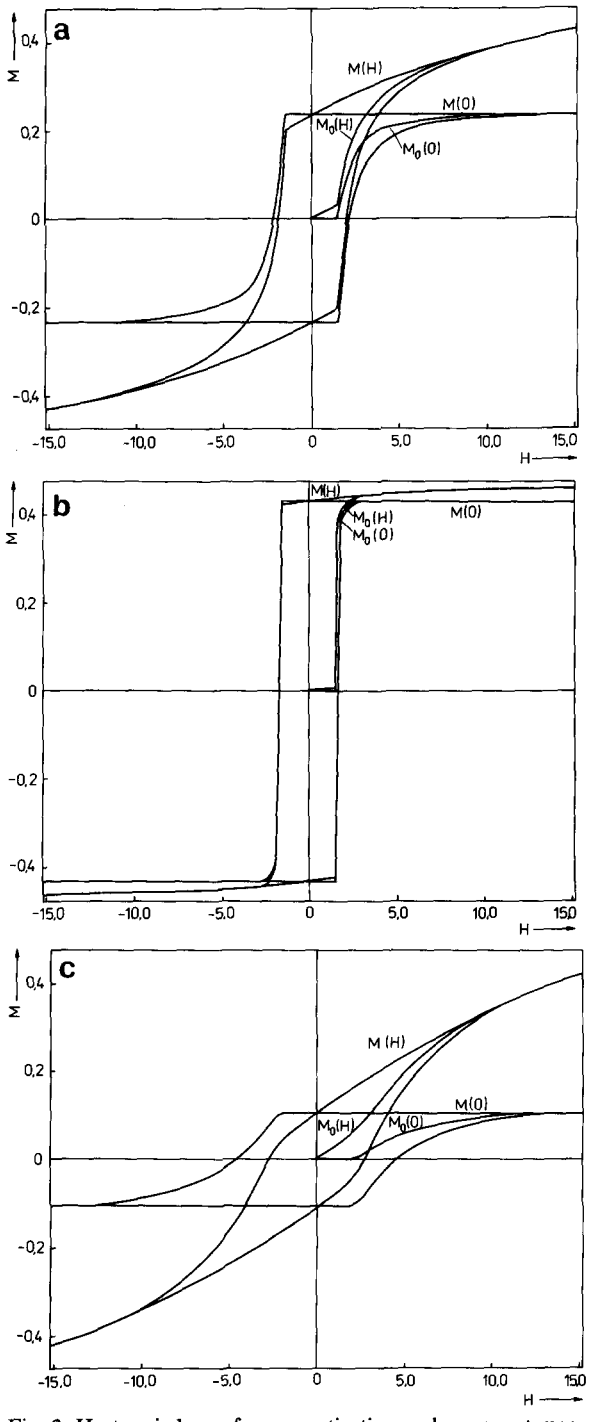

Fig. 2. Hysteresis loops for magnetization and remanent magnetization with the corresponding virgin curves for different texture parameters and angles θ: (a) $n = 0$; (b) $n = 5$, $\theta = 0$; (c) $n = 5$, $\theta = \pi/2$. ($H_A = 15.1 \times 10^5$ Am^{-1}, $M_S = 0.47$ Vsm^{-2} are used in all figs.)

ent texture parameter n and for two angles θ between the texture axis and the external field. In fig. 2a for an isotropic sample ($n = 0$) the magnetization component parallel to the field $M(H)$, the corresponding remanence values $M^r = M(H = 0)$ obtained after switching off the field, and the corresponding values for the virgin curves $M_0(H)$ and $M_0(0)$ are presented.

The sharp kinks in the curves at $H = \pm H_c^0$ are due to the model assumption of a single value H_c^0 for all particle. They can be smoothed out by using a distribution of Kondorsky parameters H_c^0. For isotropic samples (fig. 2a) reversible rotation processes of the magnetization are very important where for a texture parameter $n = 5$ (fig. 2b) the hysteresis loops are already nearly rectangular. Hence in magnets with $H_c^0 \ll H_A$ a further increasing of the texture ($n > 5$) has almost no influence on the shape of the hysteresis loop for small θ.

In fig. 2c the corresponding curves are plotted for a magnetic field perpendicular to the texture axis ($\theta = \pi/2$). The calculation of hysteresis loops for arbitrary angles θ is of some practical interest since for badly texturized samples it is somewhat difficult to determine the position of the texture axis precisely.

3.2. Minor loops

The investigation of minor loops is of interest for the study of different magnetization processes. Therefore, starting from the virgin state hysteresis loops for magnetic fields $H_{max} = H_A$, $H_{max} = 2H_c^0$ and $H_{max} < H_c^0$ have been considered.

As shown in fig. 3a for an isotropic sample for $H > 2H_c^0$ the main contribution to the minor loops is given by the incoherent magnetization processes. Beginning with $H = H_A/2$ irreversible coherent remagnetization processes take place, but for that case the minor loop already bears a great resemblance to the outer hysteresis loop (fig. 3a). For higher values of n all minor loops nearly coincide already for $H \gtrsim H_c^0$.

For magnetic fields not coinciding in direction with the texture axis ($\theta \neq 0$, fig. 3b) the minor loops are more different even for a good texture. In this case the irreversible coherent magnetization processes become more important.

In fig. 4 the component $M_\perp$ transverse to the magnetic field is plotted for $n = 5$ and $\theta = \pi/4$. It should be noted that for $\theta \neq 0$ even for fields $H \geqslant H_A$ the magnetization component perpendicular to the magnetic field is quite considerable.

3.3. Virgin curves

In fig. 5a virgin curves are plotted for the magnetization and the magnetization remanence. As already noted in section 3.1 the sharp kinks at $H = H_c^0$ can be smoothed by taking into account a distribution of the parameter H_c^0. In fig. 5b the corresponding curves are shown where the demag-

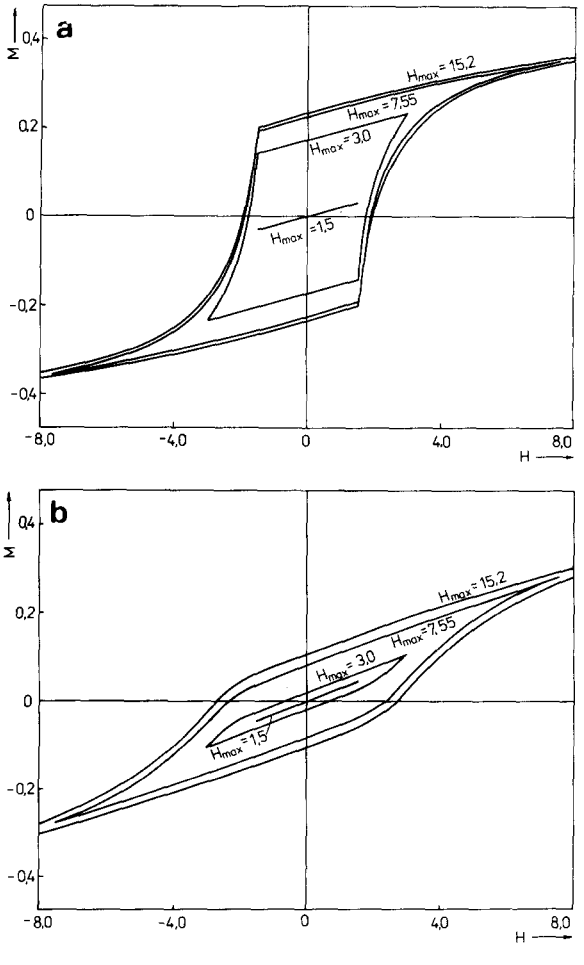

Fig. 3. Minor loops for $n = 0$ (a) and $n = 5$, $\theta = \pi/2$ (b).

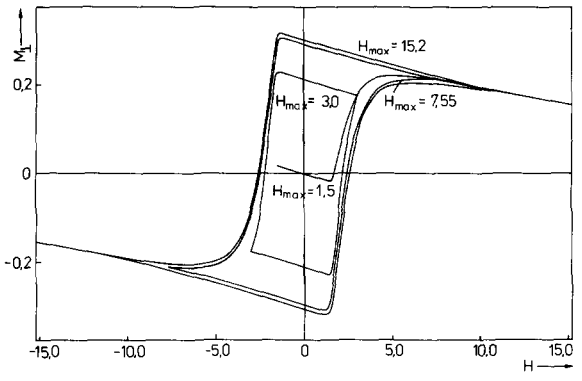

Fig. 4. Transversal component of the magnetization $M_\perp(H)$ as function of H for $n = 5$, $\theta = \pi/4$.

netized state was obtained applying an opposite field (remanence coercive field) to the saturated sample (state III). The comparison of 5a and b shows that the initial susceptibility of the field demagnetized state is larger than that of the virgin state.

The approach to magnetic saturation at fields $H \gg H_A$ can be described by expanding $M_\parallel$ in powers of (H_A/H). In the lowest order one finds

$$M_\parallel = M_S\left[1 - \left(\frac{H_A}{H}\right)^2\left(\frac{(n+1)+n(2n-1)\cos^2\theta}{(2n+3)(2n+5)} - \frac{2n(n-1)\cos^4\theta}{(2n+3)(2n+5)}\right)\right] \tag{8}$$

and the remanence (at $H \geqslant H_A$) [10]

$$M_\parallel^r = M_S\frac{2n+1}{2n+2}\left[1 - \sum_{k=0}^{n-1}\frac{(2k-1)!!}{(2k+2)!!}\sin^{2k+2}\theta\right]. \tag{9}$$

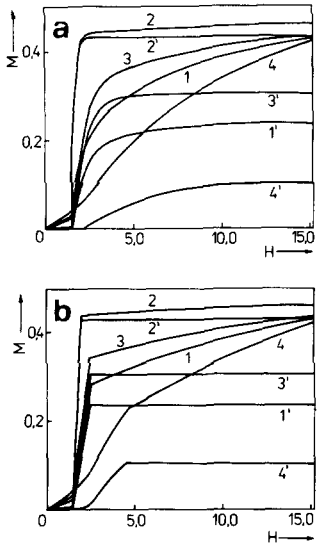

Fig. 5. Magnetization (1 to 4) and remanent magnetization (1′ to 4′) curves starting from the virgin state (a) and the field demagnetized state (b), resp.: 1, 1′ – $n = 0$; 2, 2′ – $n = 5$, $\theta = 0$; 3, 3′ – $n = 5$, $\theta = \pi/4$; 4, 4′ – $n = 5$, $\theta = \pi/2$.

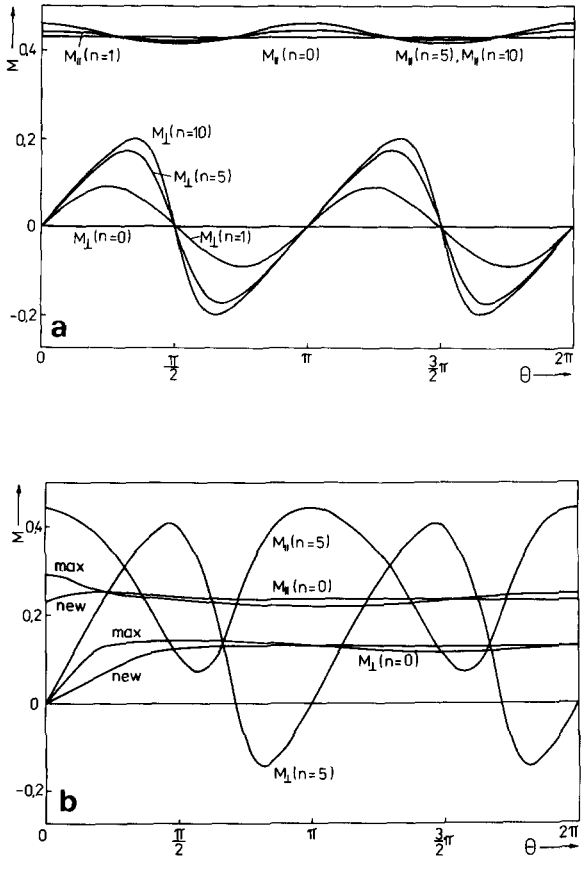

Fig. 6. Rotational hysteresis of the magnetization components parallel and perpendicular to the magnetic field $M_\parallel$ and $M_\perp$, resp., for different texture parameters n: (a) $H = H_A$; (b) $H = 2H_c^0$.

4. Rotational hysteresis

4.1. Torque curves

The investigation of rotational hysteresis gives an additional possibility of getting information on the magnetization processes. To measure the rotational hysteresis the sample rotates with respect to a constant magnetic field, and the torque $\boldsymbol{D} = \boldsymbol{M} \times \boldsymbol{H}$ is determined as a function of the angle θ. Since $|\boldsymbol{D}| \propto M_\perp$ it is sufficient to calculate $M_\perp(\theta)$, where for completeness in this paper $M_\parallel(\theta)$ is calculated, too.

In fig. 6 the components $M_\perp(\theta)$ and $M_\parallel(\theta)$ for a magnetic field $H = H_A$ (fig. 6a) and $H = 2H_c^0$ (fig. 6b), resp., for different texture parameters n are plotted. As shown in fig. 6b for fields $H < H_A$ in general the torque curves depend on the magnetic prehistory of the sample. In fig. 6b the partially magnetized initial state IV and the saturated state (cf. section 2.4.) are considered. For magnets with a high texture the influence of the initial state is negligible (cf. curve with $n = 5$).

In fig. 7a, $M_\perp$ and $M_\parallel$ are plotted for a texture parameter $n = 5$ and magnetic fields $H = 2H_c^0$, $H = H_A/2$, and $H = H_A$. For the same parameters in fig. 7b the remanent magnetizations $M_\perp^r(\theta)$ and $M_\parallel^r(\theta)$ are shown which are obtained by rotating the magnetic field to the angle θ and then switching it off. It should be noted that the relation (cf. ref. [9])

$$M_\perp^r(\theta) = -\frac{\mathrm{d}}{\mathrm{d}\theta} M_\parallel^r(\theta) \tag{10}$$

is fulfilled only for fields $H > H_A$ or $H < H_c^0$. For intermediate fields in general relation (10) is not true due to irreversible magnetization jumps at changing θ which results in a θ-dependence of the probability function $W_\nu(\alpha, \epsilon)$ in (6).

Finally in fig. 8a "slanting" torque curve is shown where $\theta_{min} = \pi/4$ is the angle between the texture axis and the plane in which the field rotates. $M_\perp$ and $M_\parallel$ are plotted as functions of θ_1 where θ_1 is the angle in the rotation plane. θ_1 is connected with θ by $\cos\theta = \cos\theta_1 \cos\theta_{min}$, and the angle ϵ as well as the expression for $M_\perp$ of (6) have to be redefined, too [10]. As discussed in

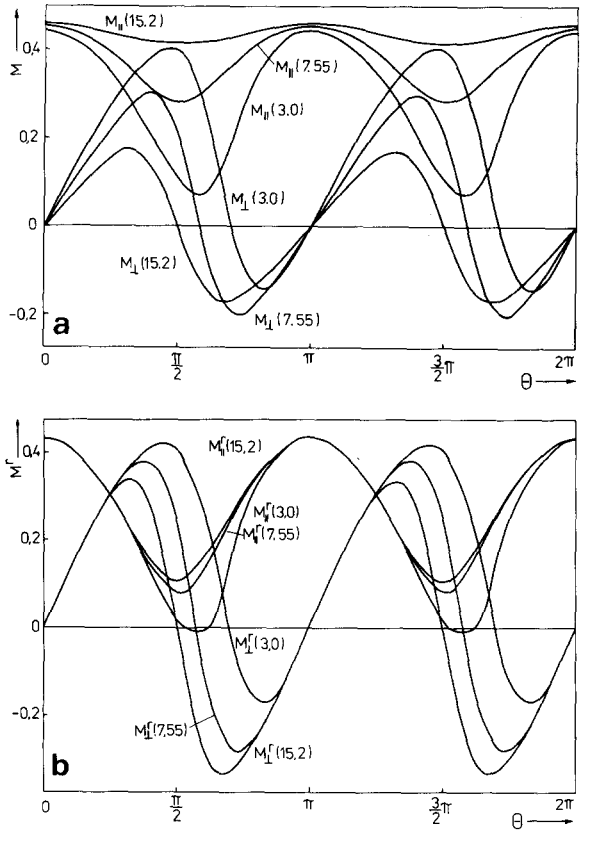

Fig. 7. Rotational hysteresis of magnetization $M_\parallel$, $M_\perp$ (a) and the remanent magnetization $M_\parallel^r$, $M_\perp^r$ (b), resp., for different magnetic fields and $n = 5$.

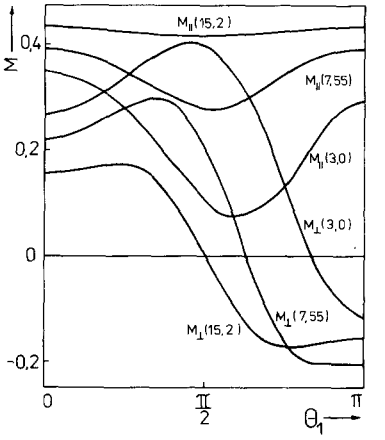

Fig. 8. "Slanting" rotational hysteresis curves of the magnetization $M_\parallel$, $M_\perp$ for different magnetic fields and $n = 5$, $\theta_{min} = \pi/4$.

section 3, "slanting" curves are of importance if the texture axis is not known exactly.

4.2. Remanence angle

The texture of a magnet can be determined quite simply by measuring the so-called remanence angle γ [11]. γ is the angle between the texture axis and the magnetization after switching off the rotating magnetic field. It is given by

$$\gamma(\theta) = \theta - \arctan\left(M_{\perp}^{r}(\theta)/M_{\parallel}^{r}(\theta)\right). \qquad (11)$$

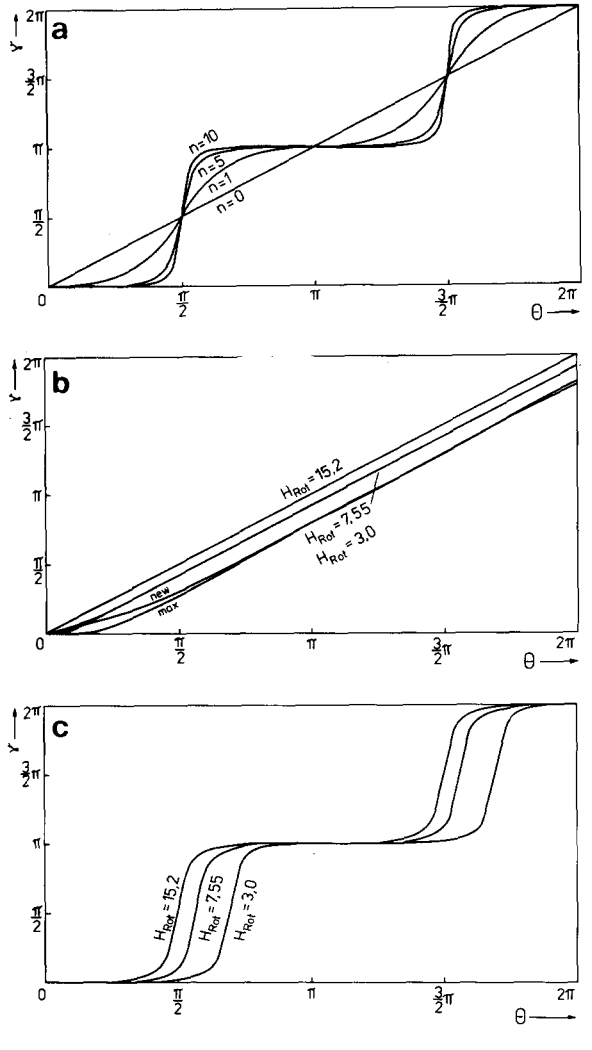

Fig. 9. Remanence angle, γ for a rotating magnetic field: (a) $H = H_A$, $n = 0, 1, 5, 10$; (b) $H = 2H_c^0$, $H_A/2$, H_A, $n = 0$; (c) $H = 2H_c^0$, $H_A/2$, H_A, $n = 5$.

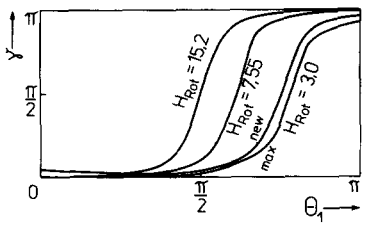

Fig. 10. Remanence angle for magnetic fields $H = 2H_c^0$, $H_A/2$, H_A rotating in a slanting plane ($\theta_{min} = \pi/4$), $n = 5$.

In fig. 9a the dependence of γ on the texture parameter n is plotted for a magnetic field $H = H_A$. For fields $H < H_A$ the remanence angle $\gamma(\pi/2)$ differs from $\pi/2$ considerably which is shown in figs. 9b and c. Hence from measurements of $\gamma(\theta)$ the anisotropy field H_A can be determined, too. Finally in fig. 10 the remanence angle is given for the "slanting" case with $\theta_{min} = \pi/4$.

5. Concluding remarks

In the present contribution, magnetization and magnetization remanence of polycrystalline samples are calculated in dependence on strength and direction of the magnetic field (hysteresis and rotational hysteresis, resp.) as well as in dependence on the prehistory of the sample (minor loops, virgin curves). The magnet is characterized by its saturation magnetization M_S, the anisotropy field H_A and the Kondorsky parameter H_c^0 of the crystallites, and the distribution of the crystallites is characterized by the texture parameter n.

The presented results are of interest for all polycrystalline magnetic materials with a high uniaxial anisotropy of the particles as, e.g., Ba- and Sr-ferrites, Sm–Co and Nd–Fe–B magnets. For definiteness in the figures the values $M_S = 0.47$ Vsm^{-2}, $H_A = 15.1 \times 10^5$ Am^{-1} (Sr-ferrites) have been used. The results can be transmitted to other materials by using relative units $m = M/M_S$, $h = H/H_A$ and $h_c^0 = H_c^0/H_A$.

In the presented calculations we put $h_c^0 = 0.1$ whereas in real systems the h_c^0 are rather distributed with a suitable distribution function. Know-

ing this distribution function, the corresponding hysteresis loops etc. can be obtained by averaging the results obtained for fixed values of h_c^0 with this function.

Acknowledgement

The authors are very indebted to Dr. L. Jahn for referring us to the experimental behaviour of polycrystalline high anisotropic materials. We thank Dr. R. Schumann for some hints concerning the numerical calculations. Finally, we would like to express our gratitude to Prof. E.P. Wohlfarth for stimulating us to carry out the presented calculations.

References

[1] L. Néel, IEEE Trans. Magn. MAG-17 (1981) 2516.
[2] Yu.L. Raikher, J. Magn. Magn. Mat. 39 (1983) 11.
[3] R.W. Chantrell, N.Y. Ayoub and J. Popplewell, J. Magn. Magn. Mat. 53 (1985) 199.
[4] L. Jahn, R. Schumann and V. Christoph, Phys. Stat. Sol. (a)88 (1985) 595.
[5] E.J. Kondorsky, Izv. Akad. Nauk (Ser. Fiz.) 16 (1952) 398.
[6] U. Heinecke, Phys. Stat. Sol. 30 (1968) 551.
[7] L.D. Livingston, J. Appl. Phys. 53 (1981) 2544.
[8] E.H. Frei, S. Shtrikman and D. Treves, J. Appl. Phys. 30 (1959) 443.
[9] H. Stäblein, Techn. Mitteilungen Krupp 24 (1966) 103.
[10] K. Elk, V. Christoph, L. Jahn and R. Schumann, Wiss. Z. HfV Dresden, to be published.
[11] L. Jahn, Dr. Thesis, Technical University Dresden (1985).